



OIST

OKINAWA INSTITUTE OF SCIENCE AND TECHNOLOGY GRADUATE UNIVERSITY
沖縄科学技術大学院大学

Dynamic control of neurochemical release with ultrasonically-sensitive nanoshell-tethered liposomes

Author	Sean M. Mackay, David Mo Aung Myint, Richard A. Easingwood, Dylan Y. Hegh, Jeffery R. Wickens, Brian I. Hyland, Guy N. L. Jameson, John N. J. Reynolds, Eng Wui Tan
journal or publication title	Communications Chemistry
volume	2
page range	122
year	2019-10-25
Publisher	Nature Research
Rights	(C) 2019 The Author(s).
Author's flag	publisher
URL	http://id.nii.ac.jp/1394/00001402/








doi: [info:doi/10.1038/s42004-019-0226-0](https://doi.org/10.1038/s42004-019-0226-0)

ARTICLE

<https://doi.org/10.1038/s42004-019-0226-0>

OPEN

Dynamic control of neurochemical release with ultrasonically-sensitive nanoshell-tethered liposomes

Sean M. Mackay ¹, David Mo Aung Myint¹, Richard A. Easingwood ^{2,3}, Dylan Y. Hegh¹,
Jeffery R. Wickens ⁴, Brian I. Hyland ⁵, Guy N.L. Jameson ^{1,6}, John N.J. Reynolds ² & Eng Wui Tan ^{1*}

The unique surface plasmon resonance of hollow gold nanoshells can be used to achieve drug release from liposomes upon laser stimulation, and adapted to mimic the intricate dynamics of neurotransmission *ex vivo* in brain preparations. However, to induce a physiological response *in vivo* requires the degree of temporal precision afforded by laser stimulation, but with a greater depth of penetration through tissue. Here we report that the attachment of hollow gold nanoshells to the surface of robust liposomes results in a construct that is highly sensitive to ultrasonic stimulation. The resulting construct can be remotely triggered by low intensity, therapeutic ultrasound. To our knowledge, this is the first example of nanoparticle-liposome system that can be activated by both laser and acoustic stimulation. The system is capable of encapsulating the neurochemical dopamine, and repeatedly releasing small amounts on-demand in a circulating environment, allowing for precise spatiotemporal control over the release profile.

¹Department of Chemistry, University of Otago, Dunedin, New Zealand. ²Department of Anatomy, University of Otago, Dunedin, New Zealand. ³Center for Electron Microscopy, University of Otago, Dunedin, New Zealand. ⁴Okinawa Institute of Science and Technology Graduate University, Okinawa, Japan. ⁵Department of Physiology, University of Otago, Dunedin, New Zealand. ⁶Present address: School of Chemistry and Bio21 Molecular Science and Biotechnology Institute, 30 Flemington Road, The University of Melbourne, Parkville 3010 Victoria, Australia. *email: ewtan@chemistry.otago.ac.nz

Advances in nanotechnology-based delivery vehicles have resulted in promising systems towards achieving drug release locally with precise temporal control. Liposomes are widely used as drug delivery systems as they possess the ability to achieve localised delivery of a therapeutic agent^{1,2}, for example, in cancer therapy, where accumulation and subsequent prolonged drug release is desired in the tumour microenvironment^{3,4}. In addition to localisation, temporal control over the release profile of a therapeutic agent would be desirable to allow for drug release that mimics natural biological patterns. Such an approach could lead to improved treatments for neurological disorders, including Parkinson's disease, where some of the movement disorder is attributed to the temporal pattern of dopamine receptor stimulation^{5,6}.

One promising nanoparticle system which allows for precise temporal control is the addition of near-infrared (NIR) absorbing hollow gold nanoshells (HGNs) to the surface of liposomes⁷. This system can be remotely activated via irradiation with a NIR laser to achieve payload release from the liposome carrier in either a near total⁷, or repeatable non-destructive manner⁸, dependent on the number of HGNs attached and laser intensity. Recently, we adapted this system to achieve sub-second release of dopamine in a manner which mimics the natural dynamics of neurotransmitter release in the brain upon femtosecond laser stimulation^{9,10}. The precision afforded by laser stimulation can repeatedly induce localised and neurochemical-dependent physiological effects. Moreover, these effects can be elicited after a month of direct implantation into neural tissue demonstrating long-term in vivo stability of the system¹⁰. This is a significant step towards potentially restoring these processes in conditions of neurological dysfunction, but remains limited by the depth of penetration of light into tissues. Ultrasound has also been used in a similar capacity for stimulating drug release from liposomes¹¹. Since laser-stimulated release from HGN–liposome systems has been attributed to a mechanism similar to that underlying ultrasound release⁷, we hypothesised that the system developed for laser use could be further developed to release using ultrasound at therapeutic frequencies.

Ultrasound is widely accepted in clinical medicine for both diagnostic and therapeutic applications, and unlike NIR light, can achieve deep penetration into mammalian tissues¹². Nearly all ultrasound-responsive drug delivery systems involve gas-containing vesicles, for example, microbubbles, which can facilitate leakage from drugs encapsulated within carrier particles in close proximity, or co-encapsulated within the microbubble itself^{13–16}. To date, however, there are few examples of methods that sensitise the delivery vehicle itself to ultrasound. Those that have been developed all involve the addition of membrane-compromising agents, such as 1,2-dioleoyl-*sn*-glycero-3-phosphoethanolamine (DOPE)¹⁷. These existing ultrasound stimulated systems have a number of limitations, namely the large size and need for co-location with the drug-containing reservoir in the case of microbubbles, and compromised membrane integrity leading to poor entrapment efficiency. Furthermore, these systems have largely been designed to achieve the total or near-total release in response to a single ultrasound application. However, to achieve in vivo restoration of neurochemical dynamics requires the development of a stable system which can incrementally release small quantities of an encapsulated agent with precise control.

Here, we demonstrate a method of increasing the susceptibility of a liposome construct to ultrasound through the attachment of nanoparticles to the surface of a stable liposome membrane. In particular, we show that tethering hollow gold nanoshells to the liposomes results in a highly sonosensitive construct and propose a mechanistic basis for the phenomenon

observed. We then show the ability of the system to release the neurochemical dopamine in a pulsatile manner within a circulating system. To our knowledge, this is the first demonstration of a liposome–nanoparticle system capable of on-demand triggered release in response to both laser⁹ and acoustic stimulation.

Results

Gold nanoshells enhance liposome ultrasound sensitivity. To investigate the effect of nanoparticles on the acoustic sensitivity of liposomes, biocompatible liposome structures containing a thiol linker moiety (tether-ready liposomes) were prepared based on a previous publication⁹, and tethered to either solid gold nanoparticles (SNPs) or HGNs. A thin-film of 1,2-dipalmitoyl-*sn*-glycero-3-phosphatidylcholine (DPPC), cholesterol, sphingomyelin, 1,2-distearoyl-*sn*-glycero-3-phosphoethanolamine-*N*-[methoxy(polyethylene glycol)-2000] (DSPE-PEG2000) and DSPE-2000-SH in a 100:5:5:4:3.5 molar ratio was prepared¹⁸, and rehydrated with phosphate buffered carboxyfluorescein (CF) (100 mM CF, 20 mM Na₂HPO₄, pH 7.4) to form a lipid suspension containing large multilamellar vesicles. Size control of the liposome suspension was achieved by extrusion through 200-nm polycarbonate membranes. Ellman's assay¹⁹ was used to quantify the number of accessible thiol moieties per liposome. The concentration of DSPE-PEG2000-SH detected was ~50% of the total DSPE-PEG2000-SH present in suspension (Supplementary Note 1, Supplementary Table 4), suggesting that the DSPE-PEG2000-SH is distributed equally between the inner and outer leaflet of the liposome membrane.

SNPs were synthesised to ~25 nm in diameter (Supplementary Fig. 1) by the commonly used citrate reduction method²⁰. HGNs (Supplementary Fig. 2) were synthesised by galvanic replacement of a silver nanoparticle template, as previously described^{7,21}. Cryo-transmission electron microscopy (cryo-TEM) and electron tomography confirmed that the HGNs were hollow in nature (Fig. 1a and inset) with a diameter of ~25–35 nm.

The nanoparticle suspensions were added periodically in 10 μ L additions to a suspension of tether-ready liposomes to achieve a nanoparticle:lipid (mg/mmol) ratio of 55:1 and 65:1 for HGN– and SNP–liposomes, respectively, which resulted in stable liposome–nanoparticle constructs containing CF. The liposome suspensions were diluted 1:10 with phosphate buffer (20 mM, pH 7.4) and left to tether for 96 h. At these ratios, ~1 or 2 nanoparticles per liposome on average was observed by cryo-TEM (Fig. 1a).

Fluorescence intensity was measured after low intensity therapeutic (1 MHz) ultrasound was applied to the diluted suspension (1 W cm⁻², 0.38 \pm 0.02 MPa, 100% duty cycle) for 4.5 s every 3 min (Fig. 1b). Application of ultrasound to liposomes caused release of small amounts of CF upon multiple 4.5 s exposures (~5% release, 30 pulses over 90 min), which was enhanced by the attachment of SNPs (~13% release, 30 pulses over 90 min). However, ultrasound applied to liposomes tethered to HGNs resulted in a large increase in the percentage of CF released when ultrasound was applied to the suspension, achieving ~65% release after an equivalent exposure period to SNP–liposomes and tether-ready liposomes. Furthermore, the profile of release appears to level off, suggesting that magnitude of release per ultrasound application is proportional to the total amount of encapsulated CF remaining within the system. In contrast, when HGNs were merely co-dispersed with liposomes without the inclusion of the DSPE-PEG2000-SH tethering agent, no difference in CF release was observed in the presence of HGNs compared with control liposomes after acoustic stimulation (Supplementary Fig. 3). No appreciable release of carboxyfluorescein was observed in the absence of ultrasound, and the

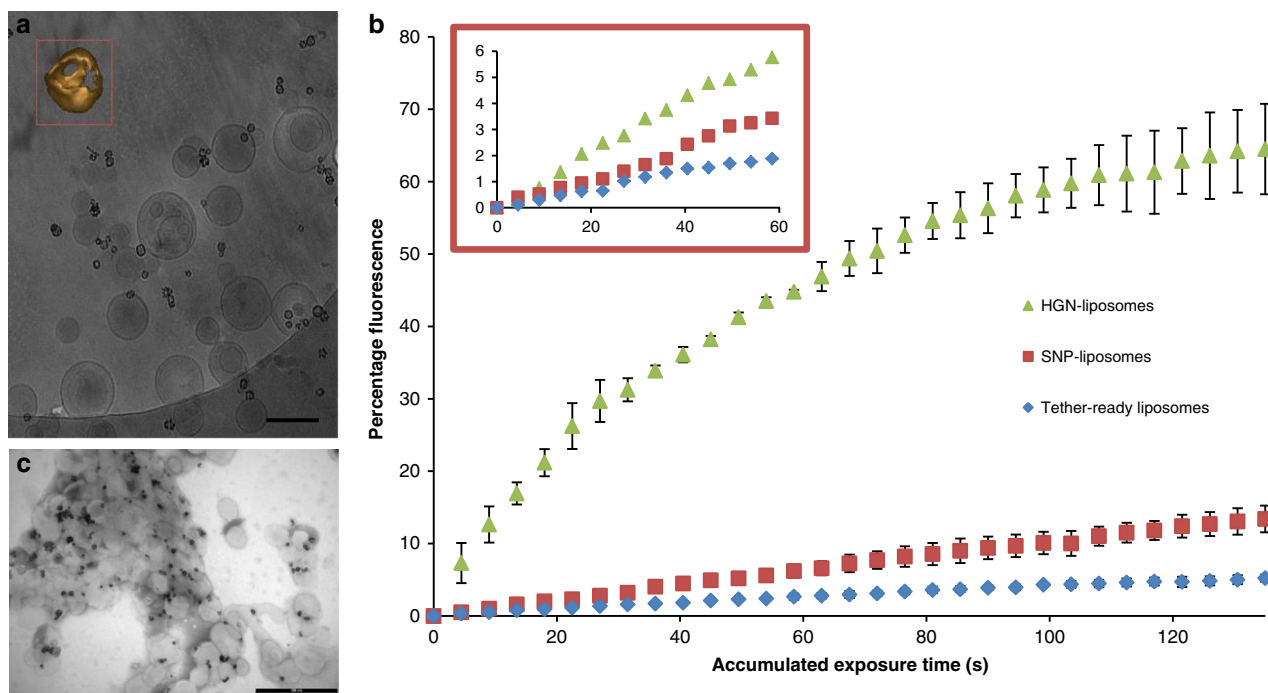


Fig. 1 Influence of gold nanoparticles on the acoustic sensitivity of liposomes. **a** Example of a cryo-transmission electron micrograph of HGN-liposomes. Red insert: An example of a 30-nm hollow gold nanoshell obtained from the image by cryo-transmission electron tomography. Scale bar = 100 nm. **b** Average (\pm standard error) percentage CF release after 96-h tethering time, measured by an increase in fluorescence intensity (ex 465, em 520 nm) upon exposure to ultrasound (4.5 s duration, every 3 min; $n = 3$ experiments; total experiment run time of ~93 min) and normalised to complete CF release by Triton X-100 for tether-ready (control) liposomes (blue diamonds), SNP-liposomes (red squares) and HGN-liposomes (green triangles). The total CF concentration in suspension after complete release is $8 \pm 1 \mu\text{M}$. Red insert: Percentage CF release after 18 h tethering time (y - and x -axis represent percentage fluorescence and accumulated exposure time (s), respectively). **c** TEM of HGN-liposomes after 100 s ultrasound application. Scale bar = 500 nm

liposomes were resistant to leakage at an elevated temperature of 34 °C over a period of 76 h ($\sim 0.2\%$ release per hour, $\sim 5\%$ after 23 h) (data not shown).

TEM of the suspensions after the period of ultrasound irradiation (Fig. 1b inset) shows that the liposome structures remain both largely intact and tethered to the HGNs, suggesting a relatively non-destructive mechanism of release. A relationship between the magnitude of CF release from HGN-tethered and SNP-tethered liposomes and tethering time appeared to exist. Sixty seconds of accumulated ultrasound exposure resulted in $\sim 3.5\%$ and 6% CF release for 18 and 96-h tethering time, and ~ 6 and 45% CF release after 18 and 96 h tethering time for SNP-liposomes and HGN-liposomes, respectively (Fig. 1b red inset). In contrast, little difference in the magnitude of release was observed in tether-ready liposomes containing no gold nanoparticles over time after the same period of applied ultrasound (2% vs 3% after 18 and 96 h). HGN-tethered liposomes have previously been shown to produce total CF release upon laser irradiation, through localised heating and subsequent cavitation at the liposome surface^{7,8,22}. However, to our knowledge, this is the first demonstration that liposomes tethered to HGNs possess a dramatically increased susceptibility to ultrasound.

Peak ultrasound sensitivity occurs with one hollow nanoshell.

The addition of HGNs to the solution of tether-ready liposomes resulted in a complex mixture of species suspended in solution, as evident by cryo-TEM of the suspensions. Therefore, it was of interest to identify which of the resulting nanoparticle-liposome conjugate species lead to the greatest enhancement in sonosensitivity. A variation of Job's method²³ was used to investigate

the liposome-nanoparticle dynamics occurring within the complex sonosensitive suspension. Increasing concentrations of HGNs were added to a fixed liposome concentration. Liposomes were prepared containing CF as previously described, however, sphingomyelin was omitted as a membrane component due to the high encapsulation efficiency of CF. Volumes of a HGN suspension (0 – $250 \mu\text{L}$; 8 mg mL^{-1} Au concentration, Supplementary Table 2) were added to equal volumes of liposome suspension and stored at 4 °C overnight (~ 18 h) for tethering to occur.

Therapeutic ultrasound was applied to each of the diluted HGN-liposome suspensions for 3 s with 3-min intervals between each application. The temperature of the suspension after ultrasonication did not change appreciably from room temperature (23 – 25 °C), well below the temperature required to initiate leakage (35 °C). A significant increase (\sim fivefold over 15 s accumulated exposure) in the amount of CF released with increasing accumulated exposure time was observed for those suspensions containing 50 and $100 \mu\text{L}$ of a HGN suspension, when compared with control liposomes containing no HGNs (Fig. 2a). However, a decreasing trend in the percentage of CF released was observed for liposome-HGN constructs containing $150 \mu\text{L}$ or more of the HGN suspension. The Z-average and polydispersity index of the suspensions also increased with HGN additions $100 \mu\text{L}$ and greater, suggesting an increase in the degree of aggregation present (Supplementary Fig. 4). An asymptotic effect on the Z-Average is observed in suspensions with $150 \mu\text{L}$ and greater, which suggests that although aggregation occurs at these ratios, the size of the aggregates may not necessarily be governed by the amount of HGNs present. It should also be noted that no peaks were observed between 20 and 40 nm in the DLS, suggesting that all HGNs were associated with liposomes

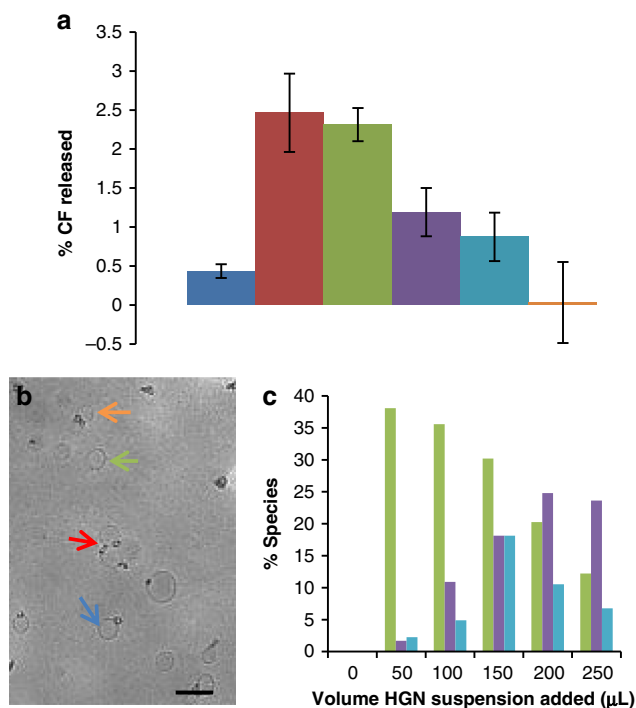


Fig. 2 Particle number influences acoustically driven release from liposomes. **a** Total cumulative CF release from liposomes tethered to 0 μL (blue), 50 μL (orange), 100 μL (grey), 150 μL (yellow), 200 μL (purple) and 250 μL (green - on x-axis) of a HGN suspension (8 mg mL^{-1}) in response to 15 s of ultrasound application (2.4 W cm^{-2} , 0.64 MPa , 100% duty cycle). The data represent average \pm standard error. The total CF concentration in suspension is $5.7 \pm 0.2 \mu\text{M}$. **b** Exemplar cryo-TEM of a suspension of HGN-liposomes indicating bare liposomes (green arrow), liposomes tethered to one HGN (blue arrow), liposomes tethered to multiple HGNS (orange arrow) and clusters of HGN-liposomes (red arrow). Scale bar = 200 nm. **c** Analysis of the relative proportions of different species present within a HGN-liposome suspension, including liposomes tethered to one HGN (grey), liposomes tethered to multiple particles (yellow), and HGN-liposome clusters (blue)

(Supplementary Fig. 5). Cryo-TEM confirmed the presence of aggregates in the higher HGN suspensions (Supplementary Fig. 6).

Figure 2b illustrates micrographs of all suspensions with incremental additions of HGNS revealed a range of species; bare liposomes, untethered HGNS, liposomes containing one tethered HGN, liposomes containing multiple tethered HGNS and HGN-liposome clusters. Figure 2c shows the quantification of species as a population percentage (details further described in Supplementary Note 2, Supplementary Tables 2 and 3). Few untethered HGN particles were evident, especially in the suspensions containing the smaller volumes of HGNS. In the suspensions displaying the greatest enhancement in sonosensitivity bare liposomes and HGN-liposomes consisting of approximately one tethered HGN particle per liposome were most evident, with clusters emerging in the 100 μL sample, which was corroborated by DLS. As the Z-average and PDI were lowest in the suspensions which displayed the greatest sensitivity to ultrasound, and as these suspensions contained the highest proportion of liposomes containing one tethered HGN, it is reasonable to assume that these criteria are critical for optimising ultrasound-induced release.

Clusters and constructs consisting of multiple HGNS per liposome were more prevalent in the suspensions with greater

HGN concentrations. Such clusters presumably form through the reaction of HGNS attached at the outer surface of the liposome membrane with unbound thiols moieties of neighbouring liposomes. The number of clusters visible by cryo-TEM appears to decrease between samples containing 150–250 μL of HGN suspension (Fig. 2c), however, the Z-average and polydispersity index of the samples show an increase within the same interval (Supplementary Fig. 4). This likely reflects an increase in the size of HGN-liposome clusters. The increase in cluster formation at higher HGN concentrations is well correlated with the observed inhibition in CF release. To investigate relationship between clustering and CF release, we extended the polyethylene glycol steric boundary by the inclusion of 1 mol% DSPE-PEG5000 in the liposome. This sufficiently prevented cluster formation with a HGN to liposome ratio of $\sim 1:1$ and resulted in an $\sim 25\%$ increase in the enhancement in sonosensitivity (Supplementary Table 1, Supplementary Fig. 7). The increased CF release observed supports our proposition that clustering inhibits ultrasound sensitivity in this HGN-liposome system.

Cryo-electron tomography of HGN-conjugated liposomes. To investigate any morphological changes to the liposome structure that may be imparted through the addition of hollow or solid gold nanoparticles, cryo-transmission electron tomography was performed on the nanoparticle-liposome conjugates (Cryo-TEM images Supplementary Fig. 8). Control liposomes with no nanoparticle conjugation displayed a typical symmetrically spherical morphology (Fig. 3aI). Co-dispersion and incubation of HGNS or SNPs with a suspension of tether-ready liposomes for 18 h resulted in successful attachment of nanoparticles to the liposome surface, confirmed by DLS by an increase in hydrodynamic diameter. Analysis of the reconstructed tomogram volumes allowed for locational analysis of the nanoparticles in relation to the liposome surface. This showed that the nanoparticles were co-located at the liposome surface in three-dimensional space, in agreement with the DLS analysis (Supplementary Fig. 5). In most cases, it was evident that HGNS were situated at a distance of $\sim 3 \text{ nm}$ from the liposome surface (Fig. 3aII). In the HGN-liposome sample after 18 h of tethering, it was also evident that in some cases, a number of particles adhered to the exterior surface of the liposome, inducing a marginal indentation into the liposome membrane (Fig. 3aIII), which became more pronounced after 96 h post conjugation (Fig. 3aIV, V). In contrast, in all cases of liposomes conjugated to two or more HGNS (Fig. 3b) and liposomes conjugated to one SNP (Fig. 3c), the conjugated nanoparticle appeared co-located with the liposome surface with a consistent space of $\sim 3\text{--}4 \text{ nm}$ at 96 h post conjugation. This morphological change observed in HGN-liposomes, but absent in SNP-liposomes, suggests a possible nanoparticle-directed membrane rearrangement and may in-part account for the enhanced acoustic sensitivity observed.

Ultrasound threshold effect of HGN-liposomes. The intensity of ultrasound applied to tissue is an important consideration for biological and clinical application. Therefore, the effect of hydrostatic pressure (and thus, mechanical index) on CF release was investigated. In general, the incidence of inertial cavitation in an ultrasonic field increases with ultrasound intensity and hydrostatic pressure²². It was hypothesised that if the addition of HGNS leads to an increase in cavitation, the enhancement effect should increase with increasing ultrasound intensity. Liposomes encapsulating CF were prepared as previously described with a tethering period of 18 h, and cryo-TEM confirmed the attachment of HGNS to tether-ready liposomes, with a ratio of approximately one HGN per liposome.

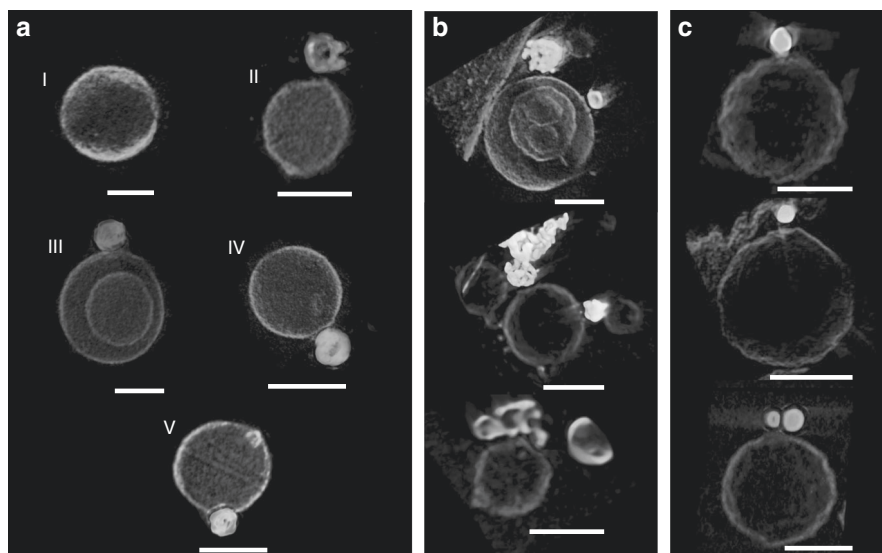


Fig. 3 Cryo-electron tomography of typical HGN-liposomes reconstructed using IMOD and Chimera software packages. **a** Control liposome (I), liposomes conjugated to one HGN after 18 h (II and III. Note that in (III) the liposome encapsulates a smaller liposome) and liposomes conjugated to one HGN after 96 h (IV and V). **b** HGN-liposomes containing two tethered HGNs after 96 h. **c** Liposomes conjugated to SNPs after 96 h. Scale bars represent 100 nm

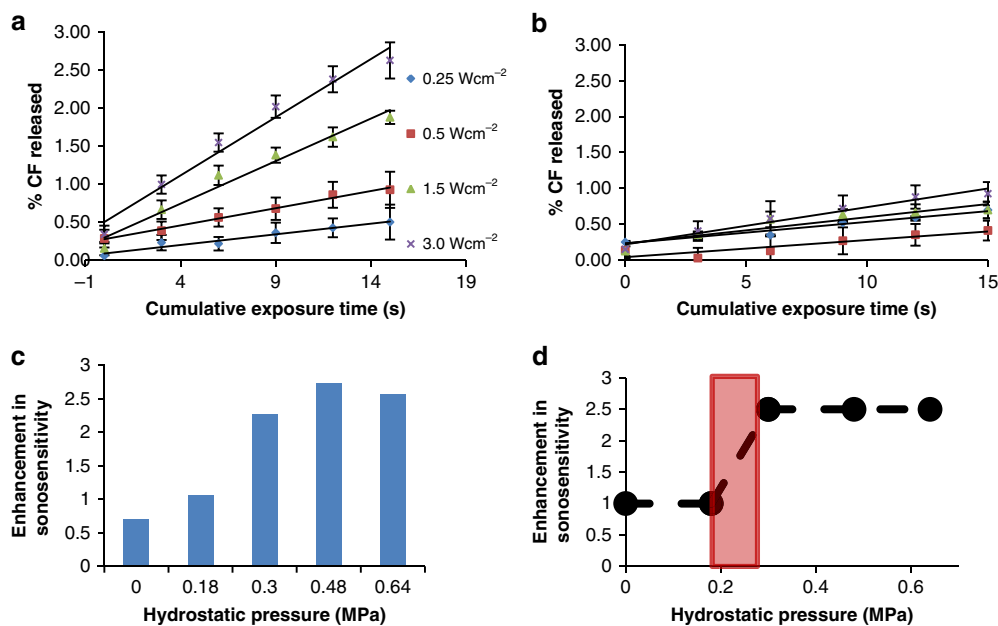


Fig. 4 Influence of acoustic pressure on release from HGN-liposomes. **a** % CF released, determined by fluorescence intensity, from HGN-conjugated liposomes and **b** control liposomes with increasing ultrasound intensities of 0.25 W cm^{-2} (blue diamonds), 0.5 W cm^{-2} (red squares), 1.5 W cm^{-2} (green triangles) and 3 W cm^{-2} (purple crosses). **c** Fold enhancement in CF release from HGN-liposomes compared with control liposomes with increasing ultrasound intensity. **d** Predicted profile for the enhancement in relative rate of CF release from HGN-tethered and control liposomes indicating the threshold acoustic pressure (red bar) required to accelerate the rate of CF release. The data represent average \pm standard error ($n = 3$). Total concentration of CF in suspension is $\sim 7.5 \pm 0.2 \mu\text{M}$

Ultrasound was applied to both control liposomes and HGN-liposomes, resulting in an increase in the percentage of CF released with increasing intensity (Fig. 4a, b). However, the percentage of CF released from control liposomes was marginal compared with that of the HGN-tethered liposomes, with maximal release reaching only 1% at an acoustic pressure of 0.64 MPa. Comparing the ratio of CF release from HGN-tethered liposomes to control liposomes revealed no apparent difference in the percentage of CF released upon irradiation with an acoustic pressure of 0.18 MPa (Fig. 4c). However, an enhancement in the sonosensitivity of HGN-tethered liposomes compared with

control liposomes was evident at acoustic pressures of 0.3, 0.48 and 0.64 MPa, which correspond to a ~ 2.5 -fold increase in the percentage of CF released from the system. This suggests that the addition of HGNs to the membrane surface decreases the acoustic energy required to elicit release, and that an ultrasound threshold energy must be met in order to observe any enhancement in sonosensitivity. Interestingly, the ratio of rate of release from HGN-tethered and control liposomes remained constant (2.5 ± 0.2 -fold) for all acoustic pressures above a clear 0.2–0.3 MPa energy threshold (Fig. 4d). As the magnitude of enhancement does not appear proportional to ultrasound intensity, this may

suggest that HGNs impart ultrasound sensitivity to liposomes in a non-cavitation manner.

On-demand spatiotemporal release of dopamine. Dopamine, an important neurotransmitter in the body and in the brain, plays multiple roles in reward and motivation^{24–26}. Abnormalities of dopamine release are associated with several diseases, including Parkinson's disease, where there is death of dopamine-containing neurons. Dopamine is normally released with very specific temporal dynamics²⁷, and so truly biomimetic replacement strategies may require similarly phasic release patterns. The ability to modulate neurochemical activity with dynamic control is currently a challenge of significant interest. Thus, our next experiments investigated the potential of our sonosensitive HGN-tethered liposome system to release dopamine in a temporally controlled manner into a circulating system designed to mimic blood flow.

Dopamine was encapsulated within liposomes using the formulation and procedure previously used for the encapsulation of CF, and stabilised against oxidation with equimolar amounts of L-ascorbic acid. Cyclic voltammetry was used to detect the concentration of non-encapsulated dopamine within the liposome suspension at an oxidation potential of ~ 0.38 V. The effectiveness of the technique was unaffected by the presence of liposomes or HGNs within the samples. A significantly higher peak in the voltammogram for each duration of ultrasound applied was detected for HGN-conjugated liposomes compared with non-tethered controls in response to ultrasound (Fig. 5a). A

linear increase in the release was observed for both HGN-tethered and tether-ready liposomes, where successive release of dopamine was sustained for prolonged ultrasound treatments, lasting over 25 individual applications (Fig. 5b).

In order to achieve minimal passive leakage of dopamine at the elevated temperatures (>35 °C) required for subsequent *ex vivo* investigations, DPPC in the lipid formulation was replaced with 1,2-distearoyl-*sn*-3-glycero-phosphatidylcholine (DSPC) due to its higher phase transition temperature. This reduced the levels of spontaneous dopamine release. *In vitro* release experiments were conducted at 35 °C with DSPC containing HGN-tethered liposomes using a flow system consisting of a liposome reservoir, peristaltic pump, ultrasound exposure chamber and recording chamber (Fig. 5c). This system was designed to simulate drug release in a flowing vascular system. The liposomes remained stable with minimal leakage throughout numerous cycles of ultrasound treatment over 2 days. Phasic micromolar increases in the concentration of dopamine in the recording chamber was achieved with repeated ultrasound exposures of 2–5 s or higher at an intensity of 2.4 W cm^{-2} (0.64 MPa ; 100% duty cycle) (Fig. 5d). No appreciable release of dopamine was observed in the absence of ultrasound over the time period of the experiment (~ 80 min for HGN-tethered liposomes and ~ 50 min for control non-tethered liposomes).

Discussion

Given the insensitivity of traditional, sub-500-nm unilamellar liposomes to shear stress²⁸ and ultrasound forces²⁹, the addition

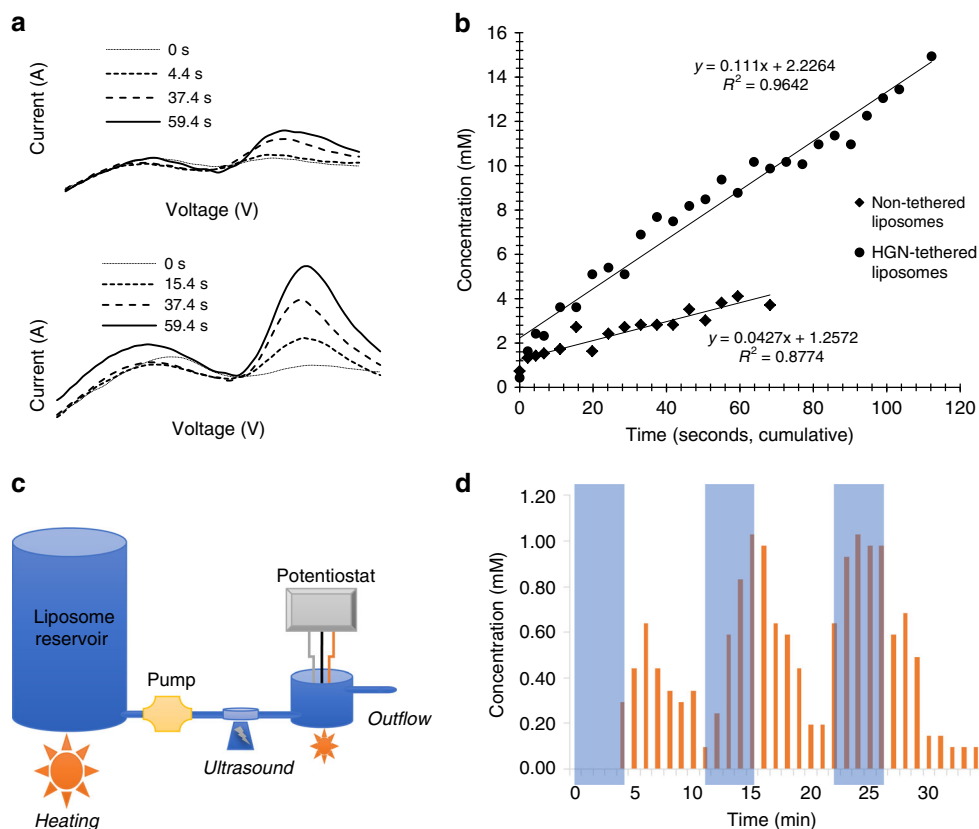


Fig. 5 Detection of dopamine by cyclic voltammetry in response to ultrasound. **a** Representative cyclic voltammograms used to verify the presence of dopamine released from liposomes. Top: non-tethered liposomes. Bottom: HGN-tethered liposomes. **b** Representative example of linear release of dopamine from HGN-tethered and non-tethered liposomes over successive ultrasound applications at 20 °C (room temperature). Note: each data point represents 2–5 s of 2.4 W cm^{-2} ultrasound exposure applied every 3 min. The total experiment run time is ~ 50 min for control non-tethered liposomes, and ~ 80 min for HGN-tethered liposomes. **c** Schematic illustration of the circulating flow system. **d** Representative example of phasic dopamine release at 35 °C in a circulating flow system. Blue bars indicate a 9 s continuous ultrasound application at 2.4 W cm^{-2} (0.64 MPa) every 20 s

of HGNs to the surface of a liposome presents a unique method of sensitising robust liposome structures to acoustic stimulation. Maximal release was achieved from monodisperse suspensions when the liposomes were conjugated to approximately one structurally hollow nanoparticle. An acoustic pressure threshold of ~ 0.2 MPa was observed to elicit CF release. This is considerably lower than that previously observed for sonosensitive liposomes containing DOPE under identical ultrasound conditions³⁰, without the need for membrane-compromising additives. In addition, release appears to occur in a primarily non-destructive manner, with evidence of intact HGN-tethered liposomes after the application of ultrasound visible by TEM. Therefore, as a consequence of these observations we believe that the primary mechanism of release in this HGN–liposome system is likely non-vascular in nature.

A relationship was observed between HGN–liposome tethering time and the subsequent susceptibility to ultrasound, which was not observed in liposomes tethered to SNPs. Cryo-electron tomography (cryo-TEM) of the liposomes tethered to one HGN or SNP over a 96-h period revealed an intriguing sequence of events. Approximately 18 h post conjugation, in most cases, a small ~ 3 – 4 -nm space was visually apparent between the liposome and the HGN or SNP surface, consistent with the length of a 2000 Da polyethylene glycol chain extending from the membrane surface at 7 mol% PEGylation³¹. Therefore, as the total degree of PEGylation (DSPE-PEG2000 and DSPE-PEG2000-SH) was 7.5 mol%, the ~ 3 – 4 -nm space between the HGN and liposome surface likely corresponds to the length of the 2000 Da polyethylene glycol chain protruding from its surface. After 96 h, HGNs in the single HGN–liposome population appeared to adhere to the liposome surface resulting in a minor indentation within the liposome membrane; a phenomenon not observed when multiple HGNs are attached to the same liposome.

Based on the time-dependant change in morphology observed in HGN–liposomes, we propose that initial rapid binding of DSPE-PEG2000-SH to a neighbouring HGN occurs, followed by slow lateral translocation of the remaining thiol-derived lipids. This results in multiple points of attachment to the single HGN and leads to stronger adherence to the lipid membrane (Fig. 6). The lateral translocation and cumulative binding of thiol-derived phospholipids would likely produce a DSPE-PEG2000-SH-enriched domain beneath the point of nanoparticle attachment. In the case where multiple HGNs are bound, each HGN would receive only a portion of the fixed number of DSPE-PEG2000-SH linkages available within the membrane, creating a weaker attraction to the liposome surface. Contrary to what might be expected, this phenomenon was absent when SNPs are used in place of HGNs demonstrating a critical requirement for the hollow nanostructure. This may result from the increased

available surface area, porosity and defects creating a more reactive surface³². It is proposed that this process of HGN-mediated phospholipid ordering may be akin to the migration of clathrin proteins during endocytosis of a particle, where diffusive mobile receptors wrap around a ligand-coated particle³³. However, due to the steric and geometric constraints of a 150–200-nm phospholipid membrane, and particularly the DSPE-PEG2000 component, the membrane wrapping of the HGN is limited to the marginal indentation observed.

Further understanding of this phenomenon can be achieved by considering the size of the spherical cap that would be occupied by co-localised DSPE-PEG2000-SH phospholipids. An estimate of the number of phospholipids in a 200-nm liposome can be made by considering the surface area of the inner and outer leaflets of the liposome, and the weighted average lipid headgroup surface area of the membrane constituents. For example, the spherical cap of a liposome directly beneath a 30-nm nanoparticle can be calculated to occupy 2900 nm² of surface area on the outer membrane leaflet. Furthermore, assuming a weighted average lipid headgroup surface area of 0.68 nm², the number of phospholipids within a 200-nm liposome would be 351580; of which 5236 are DSPE-PEG2000-SH molecules residing in the outer liposome leaflet. Due to the larger headgroup surface area of 1.4 nm²³⁴, this would occupy 7330 nm² of the liposome surface. Therefore, when only one nanoparticle is conjugated to a liposome surface, the available surface area occupied by completely agglomerated DSPE-PEG2000-SH is ~ 2.5 times that of the surface cap beneath an attached nanoparticle, enabling strong adhesion of the particle to the membrane domain, resulting in indentation of the nanoparticle into the liposome surface and discontinuity of the membrane structure. As the number of attached nanoparticles increases, the DSPE-PEG2000-SH surface area available for nanoparticle conjugation decreases, and consequently, so does the strength of nanoparticle adhesion to the DSPE-PEG2000-SH enriched domain. We propose that the increased binding interactions between a HGN to DSPE-PEG2000-SH enriched membrane domains and the resulting inhomogeneity and discontinuity of the membrane structure imparted through this phenomenon may account for the origin of acoustic sensitivity in HGN–liposome systems.

A change in volume of a lipid vesicle in response to pressure fluctuations has previously been observed and attributed to water exit from the vesicle during pressure loading³⁵. We further propose that under ultrasound conditions, pressure fluctuations would be expected to cause contraction and expansion of the liposome, albeit to a small degree dependant on the amplitude of the ultrasound wave. As a region of the external liposome surface is attached to the much more rigid gold nanoparticles surface, the resulting push–pull effect would generate shear stress at

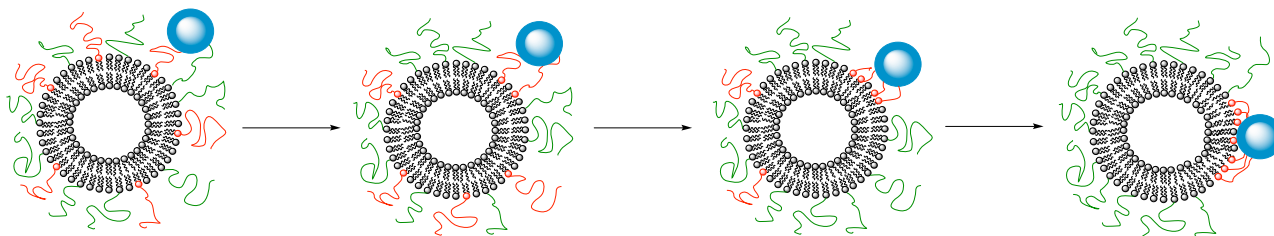


Fig. 6 Schematic illustration of the mechanism proposed for the indentation of HGNs within the liposome membrane over time. Initial binding of an HGN (blue) to a DSPE-PEG2000-SH tethering agent (red) occurs rapidly, and subsequently, lateral translocation of the remaining DSPE-PEG2000-SH linkers can occur over time, resulting in multiple binding events to the same HGN, increasing the affinity between the liposome membrane and HGN surface, ultimately resulting in an indentation of the particle within the membrane surface. Note that red phospholipids agglomerate beneath the nanoparticle to form the “spherical cap” of the liposome

the HGN–liposome interface facilitating release of the encapsulated agent. Further investigation is required to test this proposed mechanism of enhanced sonosensitivity in HGN–liposomes.

It is also interesting to note that no increase in CF release was observed in response to ultrasound when a HGN population was merely co-dispersed with a liposome suspension without the inclusion of a thiol-derived phospholipid, unlike that observed by Wu et al. when investigating laser triggered release of CF from HGN-conjugated liposomes⁷. This phenomenon was attributed to rapid heating of the HGNS, resulting in the transient formation and collapse of vapour bubbles in the surrounding solution occurring within the diffusional vicinity of neighbouring untethered liposomes. In addition, other nanoparticle systems have been used as cavitation nuclei, eliciting release from co-dispersed liposomes within proximity of the peak bubble diameter of the cavitation event^{36–40}. Given that no release was observed from liposomes co-dispersed with HGNS in this study, it is postulated that the primary mechanism of release may be non-cavitation in nature, and rather the result of acoustic pressure and shear forces disrupting the boundary of a DSPE-PEG2000-SH-enriched lipid domain beneath the point of nanoparticle attachment, possibly leading to transient pore formation and release^{34,41,42}.

We have demonstrated incremental release of encapsulated agents over prolonged periods of ultrasound application, and recorded phasic changes in dopamine concentrations within a circulating system. Phasic as opposed to continuous release of bioactive agents has implications for the improved treatment of a variety of diseases, including cancer⁴³, osteoporosis^{44,45} and neurological disorders¹⁰. Existing ultrasound and NIR-releasing systems, such as DOPE liposomes¹⁷ and pramipexole PLGA microspheres⁴⁶, use minutes of stimulus to create phasic or step-wise concentration changes on an hour timescale. In contrast, the HGN–liposome system can be activated with both NIR^{9,10} and ultrasound stimuli on a second timescale to create burst concentrations lasting for seconds to minutes. This timescale and release profile is comparable with the rhythmic release of neurotransmitters and neuromodulators in the brain^{47,48}. We envisage this nanoparticle system functioning as an inertly circulating drug reservoir which is intravenously injected, and activated via focal application of ultrasound. Upon activation with temporally controlled ultrasonic pulses, repeated bursts of blood–brain–barrier permeable neurochemical modulators are released into the brain vasculature, cross the blood–brain barrier and elicit or restore an appropriate neurochemical response. Our future intent is to demonstrate the applicability of this technology in controlling neurochemical activity in vivo in models of neurological disease, initially using models of epilepsy and Parkinson's disease. This system is anticipated to be well-tolerated as liposomes are biocompatible and HGNS have to-date demonstrated minimal cytotoxicity⁴⁹ and have been shown to break down in human blood serum³², providing a potential pathway for degradation and elimination. The development of drug-release technologies that can accurately mimic these temporal profiles may provide a new avenue towards biomimetic therapeutics, where the release profile of the therapeutic agent can be tailored to interface with an endogenous process and restore normal function.

Methods

Preparation of liposomal nanostructures. All chemicals and drugs were purchased from Sigma Aldrich, and phospholipids from Avanti Polar Lipids and Laysan Bio, and used without further purification or modification. Carboxy-fluorescein was purchased from Molekula. Hollow gold nanoshells were prepared as per a previously reported procedure by Prevo et al.²⁰. Solid gold nanoparticles were prepared via the citrate reduction method, as previously described by Marinakos et al.¹⁹. Both nanoparticle suspensions were stabilised to aggregation by surface derivatization with a 750 Da thiol-derived polyethylene glycol at a ratio of

~1:7 and 1:10 mmol/mmol for HGNS and SNPs, respectively, and concentrated by centrifugation at 10,000 rcf. All final concentrated gold nanoparticle suspensions were analysed by inductively coupled plasma mass spectrometry (ICP-MS) to quantify the total gold concentration in the suspension. The 750 Da thiol-derived polyethylene glycol was synthesised through the reaction of methoxypolyethylene glycol amine (750 Da) with 2-iminothiolane in a 1:2 mol ratio in 3 mM sodium phosphate buffer at pH 9.3. The thiol-derived DSPE-PEG-2000 phospholipid used for nanoparticle conjugation as previously described from 1,2-distearoyl-*sn*-glycero-3-phosphoethanolamine-*N*-[amino(polyethylene glycol)-2000] (sodium salt) (DSPE-PEG2000-NH₂) using 2-iminothiolane in a 1:2 mol ratio in 3 mM phosphate buffer at pH 9.3⁹.

Liposomal nanostructures were prepared using the thin-film rehydration method as previously described, using a phospholipid composition comprising either 1,2-dipalmitoyl-*sn*-glycero-3-phosphocholine (DPPC) or 1,2-distearoyl-*sn*-glycero-3-phosphocholine (DSPC) with cholesterol, sphingomyelin, DSPE-PEG2000 and DSPE-PEG2000-SH in a 100:5:5:4:3.5 mol ratio^{9,10}. The lipid components were dissolved in chloroform, combined in the appropriate ratios and the solvent removed in vacuo to form a lipid film. The film was then re-suspended using the appropriate volume of an aqueous solution containing phosphate buffer (20 mM Na₂HPO₄, pH 7.4) containing carboxyfluorescein, dopamine or apomorphine. In the case of dopamine or apomorphine, ascorbic acid (2 mg mL⁻¹) or sodium metabisulfite (1 mg mL⁻¹) was included in the aqueous solution to prevent oxidation of the bioactive agent. The phospholipid suspension was extruded 15 times through 200-nm polycarbonate membranes to achieve size-controlled unilamellar vesicles. Excess dye or drug was subsequently removed via dialysis. All samples were subjected to DLS analysis after manufacture and before use to characterise size distribution and stability to aggregation.

General procedure for ultrasound release studies in vitro. Ultrasound release studies were performed measuring the percentage fluorescence of self-quenching fluorophore carboxyfluorescein on a Perkin-Elmer LS50B luminescence spectrometer, using an excitation wavelength of 465 nm, emission wavelength of 520 nm, slit width of 2.5 nm and integration time of 0.5 s. Fluorescence intensity measurements were recorded in a 3 × 1 quartz fluorescence cuvette at a scattering angle of 90° containing 3 mL of a dilute liposome suspension (1 μM phospholipid concentration). The initial fluorescence intensity as measured over 30 s. Ultrasound was then applied to face of the cuvette at various intensities, coupled to the transducer with Aquasonic® ultrasound transmission gel and the fluorescence intensity post-application subsequently measured. To obtain the final fluorescence intensity, 100 μL of Triton-X100 (10% v/v) was added to the suspension. All release experiments were performed at room temperature using liposomes composed of the DPPC formulation. The percentage of CF released was determined by a change in fluorescence intensity, and calculated as described below:

$$\%CF \text{ Released} = \frac{I - I_0}{I_{\infty} - I_0} \quad (1)$$

where I_0 is the initial fluorescence intensity at $t = 0$, and I_{∞} is the fluorescence intensity after total liposome lysis via the addition of Triton-X100.

Dopamine release was quantified by cyclic voltammetry. A nafion-coated carbon fibre microelectrode (CFN30-1000) was used in conjunction with an CompactStat potentiostat (Ivium Technologies, Netherlands) to measure dopamine concentrations. A platinum counter electrode and an Ag/AgCl₂ reference electrode were also used. Cyclic voltammetry was performed at 0.5 V s⁻¹ for five cycles in each measurement. Baseline was subtracted from the voltammograms to measure the height of peaks associated with dopamine oxidation. The baseline was the voltammogram of HEPES buffer. Liposome suspensions (7–10 mL) were placed in a sample tube and treated with ultrasound (1 MHz, 3.0 W cm⁻²) for durations of 4.4 s per application. After each treatment, the electrodes were immersed into the liposome suspensions for measurement, and subsequently removed prior to the next application of ultrasound. All release studies were performed at 35 °C using liposomes composed of the DSPC formulation.

Electron microscopy and electron tomography. Conventional room temperature TEM was used to image the isolated HGN and SNP preparations. A suspension of the HGNS or SNPs in deionized water was applied to a carbon-coated copper mesh grid and blotted. Images were captured using a Phillips CM100 transmission electron microscope (Phillips Electron Optics, Eindhoven, The Netherlands), fitted with a MegaView 3 camera (Soft Imaging System, GmbH, Münster, Germany).

Liposome–NP conjugates were observed by cryo-TEM, using a JEOL JEM-2200FS transmission electron microscope with an omega energy filter (JEOL Ltd., Tokyo, Japan) and a Gatan 914 high-tilt cryo sample holder (Gatan Inc., CA, USA). Specimens were prepared by adding 4 μL of the diluted liposome–NP suspension to a Quantifoil® R2/2 sample grid, which had been rendered hydrophilic using a BioRad E5100 SEM coating system modified in-house for glow discharging (BioRad Microscience Ltd., Hertfordshire, UK). Excess sample was removed by blotting the grid using the filter paper. The sample was then immediately plunge-frozen into liquid ethane using a Reichert-Jung KF80 plunge freezing device (Reichert Optische Werk AG, Vienna, Austria). The frozen samples were stored under liquid nitrogen until viewing. Zero-loss energy filtered images were recorded on the JEOL TEM using a TVIPS F416 CMOS camera (TVIPS GmbH, Germany).

Data acquisition, including tilt series acquisition, was performed using Serial-EM software, and the data processed using IMOD (Boulder Laboratory for 3-D Microscopy, Colorado, USA), and Chimera (University of California San Francisco, California, USA) software packages.

Data availability

All data are available from the corresponding author upon reasonable request.

Received: 25 July 2019; Accepted: 1 October 2019;

Published online: 25 October 2019

References

- Allen, T. M. & Cullis, P. R. Liposomal drug delivery systems: from concept to clinical applications. *Adv. Drug Deliv. Rev.* **65**, 36–48 (2013).
- Torchilin, V. P. Recent advances with liposomes as pharmaceutical carriers. *Nat. Rev. Drug Disco.* **4**, 145–160 (2005).
- Peer, D. et al. Nanocarriers as an emerging platform for cancer therapy. *Nat. Nano* **2**, 751–760 (2007).
- Arap, W., Pasqualini, R. & Ruoslahti, E. Cancer treatment by targeted drug delivery to tumor vasculature in a mouse model. *Science* **279**, 377–380 (1998).
- Bibbiani, F., Costantini, L. C., Patel, R. & Chase, T. N. Continuous dopaminergic stimulation reduces risk of motor complications in parkinsonian primates. *Exp. Neurol.* **192**, 73–78 (2005).
- Thanvi, B., Lo, N. & Robinson, T. Levodopa-induced dyskinesia in Parkinson's disease: clinical features, pathogenesis, prevention and treatment. *Postgrad. Med. J.* **83**, 384–388 (2007).
- Wu, G. et al. Remotely triggered liposome release by near-infrared light absorption via hollow gold nanoshells. *J. Am. Chem. Soc.* **130**, 8175–8177 (2008).
- Forbes, N., Pallaoro, A., Reich, N. O. & Zasadzinski, J. A. Rapid, reversible release from thermosensitive liposomes triggered by near-infrared light. *Part. Part. Syst. Charact.* **31**, 1158–1167 (2014).
- Nakano, T. et al. Mimicking subsecond neurotransmitter dynamics with femtosecond laser stimulated nanosystems. *Sci. Rep.* **4**, 5398 (2014).
- Nakano, T., Mackay, S. M., Wui Tan, E., Dani, K. M. & Wickens, J. Interfacing with neural activity via femtosecond laser stimulation of drug-encapsulating liposomal nanostructures. *eNeuro* **3**, ENEURO.0107-16.2016 (2016).
- Pitt, W. G., Husseini, G. A. & Staples, B. J. Ultrasonic drug delivery—a general review. *Expert Opin. Drug Deliv.* **1**, 37–56 (2004).
- Schroeder, A., Kost, J. & Barenholz, Y. Ultrasound, liposomes, and drug delivery: principles for using ultrasound to control the release of drugs from liposomes. *Chem. Phys. Lipids* **162**, 1–16 (2009).
- Mura, S., Nicolas, J. & Couvreur, P. Stimuli-responsive nanocarriers for drug delivery. *Nat. Mater.* **12**, 991–1003 (2013).
- Ting, C.-Y. et al. Concurrent blood–brain barrier opening and local drug delivery using drug-carrying microbubbles and focused ultrasound for brain glioma treatment. *Biomaterials* **33**, 704–712 (2012).
- Bhatnagar, S., Schiffter, H. & Coussios, C.-C. Exploitation of acoustic cavitation-induced microstreaming to enhance molecular transport. *J. Pharm. Sci.* **103**, 1903–1912 (2014).
- Mears, S. & Alonso, A. Ultrasound, microbubbles and the blood–brain barrier. *Prog. Biophys. Mol. Biol.* **93**, 354–362 (2007).
- Evjen, T. J., Hagtvet, E., Nilssen, E. A., Brandl, M. & Fossheim, S. L. Sonosensitive dioleoylphosphatidylethanolamine-containing liposomes with prolonged blood circulation time of doxorubicin. *Eur. J. Pharm. Sci.* **43**, 318–324 (2011).
- Zhang, H. Thin-film hydration followed by extrusion method for liposome preparation. In *Liposomes: Methods and Protocols* (ed. D'Souza, G. G. M.) 17–22 (Springer New York, New York, 2017).
- Ellman, G. L. Tissue sulfhydryl groups. *Arch. Biochem. Biophys.* **82**, 70–77 (1959).
- Marinakos, S. M., Chen, S. & Chilkoti, A. Plasmonic detection of a model analyte in serum by a gold nanorod sensor. *Anal. Chem.* **79**, 5278–5283 (2007).
- Prevo, B. G., Esakoff, S. A., Mikhailovsky, A. & Zasadzinski, J. A. Scalable routes to gold nanoshells with tunable sizes and response to near-infrared pulsed-laser irradiation. *Small* **4**, 1183–1195 (2008).
- Forbes, N., Shin, J. E., Ogunyankin, M. & Zasadzinski, J. A. Inside-outside self-assembly of light-activated fast-release liposomes. *Phys. Chem. Chem. Phys.* **17**, 15569–15578 (2015).
- Renny, J. S., Tomasevich, L. L., Tallmudge, E. H. & Collum, D. B. Method of continuous variations: applications of job plots to the study of molecular associations in organometallic chemistry. *Angew. Chem. Int. Ed.* **52**, 11998–12013 (2013).
- Arbuthnot, G. W. & Wickens, J. Space, time and dopamine. *Trends Neurosci.* **30**, 62–69 (2007).
- Bromberg-Martin, E. S., Matsumoto, M. & Hikosaka, O. Dopamine in motivational control: rewarding, aversive, and alerting. *Neuron* **68**, 815–834 (2010).
- Flagel, S. B. et al. A selective role for dopamine in stimulus–reward learning. *Nature* **469**, 53 (2010).
- Jennings, K. A. A Comparison of the subsecond dynamics of neurotransmission of dopamine and serotonin. *ACS Chem. Neurosci.* **4**, 704–714 (2013).
- Holme, M. N. et al. Shear-stress sensitive lenticular vesicles for targeted drug delivery. *Nat. Nano* **7**, 536–543 (2012).
- Kang, M., Huang, G. & Leal, C. Role of lipid polymorphism in acoustically sensitive liposomes. *Soft Matter* **10**, 8846–8854 (2014).
- Hinow, P. et al. Signaled drug delivery and transport across the blood–brain barrier. *J. Liposome Reseach* **26**, 233–245 (2016).
- Shimada, K. et al. Determination of the thickness of the fixed aqueous layer around polyethyleneglycol-coated liposomes. *J. Drug Target.* **3**, 283–289 (1995).
- Goodman, A. M. et al. The surprising *in vivo* instability of near-IR-absorbing hollow Au–Ag nanoshells. *ACS Nano* **8**, 3222–3231 (2014).
- Gao, H., Shi, W. & Freund, L. B. Mechanics of receptor-mediated endocytosis. *PNAS* **102**, 9469–9474 (2005).
- Stepniewski, M. et al. Study of PEGylated lipid layers as a model for PEGylated liposome surfaces: molecular dynamics simulation and langmuir monolayer studies. *Langmuir* **27**, 7788–7798 (2011).
- Beney, L., Perrier-Cornet, J.-M., Hayert, M. & Gervais, P. Shape modification of phospholipid vesicles induced by high pressure: influence of bilayer compressibility. *Biophysical J., Biophysical Soc.* **72**, 1258–1263 (1997).
- Wagstaffe, S. J., Schiffter, H. A., Arora, M. & Coussios, C.-C. Sonosensitive nanoparticles for controlled instigation of cavitation and drug delivery by ultrasound. *AIP Conf. Proc.* **1481**, 426–431 (2012).
- Kwan, J. J., Graham, S. & Coussios, C. C. Inertial cavitation at the nanoscale. *Proc. Meet. Acoust.* **19**, 075031 (2013).
- Carlisle, R. & Coussios, C.-C. Mechanical approaches to oncological drug delivery. *Therapeutic Deliv.* **4**, 1213–1215 (2013).
- Kwan, J. J. et al. Ultrasound-propelled nanocups for drug delivery. *Small* **11**, 5305–5314 (2015).
- Kwan, J. J. et al. Ultrasound-induced inertial cavitation from gas-stabilizing nanoparticles. *Phys. Rev. E* **92**, 023019 (2015).
- Small, E. F., Willy, M. C., Lewin, P. A. & Wrenn, S. P. Ultrasound-induced transport across lipid bilayers: Influence of phase behavior. *Colloids Surf. A: Physicochemical Eng. Asp.* **390**, 40–47 (2011).
- Small, E. F., Dan, N. R. & Wrenn, S. P. Low-frequency ultrasound-induced transport across non-raft-forming ternary lipid bilayers. *Langmuir* **28**, 14364–14372 (2012).
- Huebsch, N. et al. Ultrasound-triggered disruption and self-healing of reversibly cross-linked hydrogels for drug delivery and enhanced chemotherapy. *Proc. Natl Acad. Sci. USA* **111**, 9762–9767 (2014).
- Dang, M., Koh, A. J., Danciu, T., McCauley, L. K. & Ma, P. X. Preprogrammed long-term systemic pulsatile delivery of parathyroid hormone to strengthen bone. *Adv. Healthc. Mater.* **6**, 1600901 (2017).
- Dang, M., Koh, A. J., Jin, X., McCauley, L. K. & Ma, P. X. Local pulsatile PTH delivery regenerates bone defects via enhanced bone remodeling in a cell-free scaffold. *Biomaterials* **114**, 1–9 (2017).
- Li, S. et al. Near-infrared light-responsive, pramipexole-loaded biodegradable PLGA microspheres for therapeutic use in Parkinson's disease. *Eur. J. Pharmaceutics Biopharmaceutics* **141**, 1–11 (2019).
- Roitman, M. F., Stuber, G. D., Phillips, P. E. M., Wightman, R. M. & Carelli, R. M. Dopamine operates as a subsecond modulator of food seeking. *J. Neurosci.* **24**, 1265–1271 (2004).
- Wickens, J. R., Budd, C. S., Hyland, B. I. & Arbuthnot, G. W. Striatal contributions to reward and decision making: making sense of regional variations in a reiterated processing matrix. *Ann. New Y. Acad. Sci.* **1104**, 192–202 (2007).
- Gu, C. et al. *In vitro* effects of hollow gold nanoshells on human aortic endothelial cells. *Nanoscale Res. Lett.* **11**, 397 (2016).

Acknowledgements

We thank the Otago Centre for Electron Microscopy TEM assistance, and David Barr, Trace Elements Centre, University of Otago, for assistance with ICP-MS. S.M.M. received a University of Otago Doctoral Scholarship. J.N.J.R. received a Rutherford Discovery Fellowship from the Royal Society of New Zealand. Funding was provided by grants from the Foundation of Research, Science and Technology; the Ministry of Science and Innovation (NERF Grant no. UOOX0807); the Ministry of Business, Innovation and Employment (Smart Ideas Phase 1; No. UOOX1403), the Otago Medical Research Foundation and Otago Innovation Ltd.

Author contributions

S.M.M. synthesised the materials, designed and performed the in vitro release experiments, performed the cryo-TEM and electron tomography, analysed and interpreted data, and wrote the paper. D.M.A.M. designed and performed the in vitro dopamine release experiments and analysed and interpreted data. D.Y.H. contributed to the synthesis of materials. R.A.E. provided technical assistance and expertise with T.E.M. and electron tomography. J.R.W., B.I.H. and G.N.L.J. contributed to concept design and provided intellectual input. J.N.J.R. and E.W.T. designed experiments, analysed and interpreted the results, edited the paper and supervised the study. All authors approved the final paper.

Competing interests

The acoustically driven drug delivery technology is described in patent application PCT/NZ2016/050130, for which J.N.J.R., E.W.T., B.I.H., G.N.L.J., D.M.A.M., S.M.M. and J.R.W. are co-inventors. All other authors declare no competing interests.

Additional information

Supplementary information is available for this paper at <https://doi.org/10.1038/s42004-019-0226-0>.

Correspondence and requests for materials should be addressed to E.W.T.

Reprints and permission information is available at <http://www.nature.com/reprints>

Publisher's note Springer Nature remains neutral with regard to jurisdictional claims in published maps and institutional affiliations.



Open Access This article is licensed under a Creative Commons Attribution 4.0 International License, which permits use, sharing, adaptation, distribution and reproduction in any medium or format, as long as you give appropriate credit to the original author(s) and the source, provide a link to the Creative Commons license, and indicate if changes were made. The images or other third party material in this article are included in the article's Creative Commons license, unless indicated otherwise in a credit line to the material. If material is not included in the article's Creative Commons license and your intended use is not permitted by statutory regulation or exceeds the permitted use, you will need to obtain permission directly from the copyright holder. To view a copy of this license, visit <http://creativecommons.org/licenses/by/4.0/>.

© The Author(s) 2019